Bioorganic Chemistry 84 (2019) 505–510

Contents lists available at ScienceDirect

Bioorganic Chemistry

journal homepage: www.elsevier.com/locate/bioorg

Bioactive butylphthalide derivatives from *Ligusticum chuanxiong*

Xu Zhang, Zi-ming Feng, Ya-nan Yang, Jian-shuang Jiang, Pei-cheng Zhang*

State Key Laboratory of Bioactive Substance and Function of Natural Medicines, Institute of Materia Medica, Chinese Academy of Medical Sciences and Peking Union Medical College, Beijing 100050, People's Republic of China

ARTICLE INFO

Keywords:
Ligusticum chuanxiong
Butylphthalide derivatives
Structure elucidation
Hepatoprotective activity

ABSTRACT

Seven new butylphthalide derivatives, ligusticumolide A-G (**1**–**7**), together with two known butylphthalide derivatives (**8**–**9**) were isolated from an ethanol extract of *Ligusticum chuanxiong* Hort. The structures of these derivatives were elucidated from analysis of 1D/2D NMR, UV, IR and HRESIMS data. The absolute configurations of these derivatives were determined by electronic circular dichroism (ECD) calculations and Mosher's method. Ligusticumolide A (**1**) and ligusticumolide B (**2**) are enantiomers that were obtained by chiral separation. Ligusticumolide C (**3**) and ligusticumolide D (**4**) are diastereomers. All of the compounds were evaluated for their hepatoprotective activity against *N*-acetyl-*p*-aminophenol-induced HepG2 cell injury. Compounds **4**, **5**, and **7**–**9** showed more significant hepatoprotective activity than that of the positive control drug (bicyclol) at a concentration of 10 μM ($p < 0.01$).

1. Introduction

Phthalides are famous bioactive compounds that are widely distributed in plants and fungi [1]. Butylphthalides represent a considerable proportion of phthalides. Previously, most of butylphthalides and their derivatives have been obtained from plants. The most representative plants are *Ligusticum chuanxiong* and *Angelica sinensis*. Hundreds of butylphthalides have been isolated from these species in the form of monomers and polymers [1,2].

In ancient China, butylphthalide-containing plants, such as *Ligusticum chuanxiong* (named Chuanxiong in China), have been widely used to treat cerebro- and cardio-vascular diseases and female irregular menstruation [3]. Modern pharmacological studies have indicated that butylphthalides such as NBP (*n*-Butylphthalide) have significant effects on cardiovascular diseases [4]. Phytochemical research indicated that butylphthalides, alkaloids and phenylpropanoids were the main bioactive compounds of *Ligusticum chuanxiong* [2,5–13]. In our previous reports, sugar-containing butylphthalides were obtained and the potential neuroprotective activity of ligusticumside A was confirmed [11]. On this basis, further phytochemical research on the liposoluble fraction was conducted. Here, seven new butylphthalide derivatives, ligusticumolide A-G (**1**–**7**), together with two known butylphthalide derivatives were isolated from the rhizome of *Ligusticum chuanxiong* Hort (Fig. 1). Evaluation of the neuroprotective activity of the compounds did not reveal potent activity. However, compounds **4**, **5**, and **7**–**9** showed significant hepatoprotective activity against *N*-acetyl-*p*-aminophenol-induced HepG2 cell injury.

2. Experimental

2.1. General experimental procedures

The optical rotations, UV spectra and ECD spectra were recorded with JASCO P-2000, V650 and J-815 spectrometers (JASCO, Easton, MD, USA), respectively. The infrared spectra were measured on a Nicolet 5700 spectrometer (Thermo Scientific, Waltham, MA, USA). The NMR spectra were recorded with a Bruker 500 MHz (Bruker-Biospin, Billerica, MA, USA). HRESIMS reports were obtained from an Agilent 6520 HPLC-Q-TOF (Agilent Technologies, Waldbronn, Germany) and LCMS-IT-TOF system (Shimadzu Scientific Instruments Inc., Kyoto, Japan). Preparative HPLC separations were performed using a Shimadzu LC-10AT with an ODS-A column (250 mm × 10 mm, 5 μm; YMC Corp., Kyoto, Japan). An Agilent 1200 series system with an Apollo C_{18} column (250 mm × 4.6 mm, 5 μm; Alltech Corp., KY, USA) was used for HPLC-DAD analysis. A Chiralpak AD-RH chiral column (250 mm × 10 mm, 5 μm; Daicel Corp., Tokyo, Japan) was used for chiral separation. Macroporous resin (Diaion HP-20, Mitsubishi Chemical Corp., Tokyo, Japan), RP-C18 (50 μm, YMC Corp., Kyoto, Japan), and Sephadex LH-20 (Pharmacia Fine Chemicals, Uppsala, Sweden) were used for column chromatography.

* Corresponding author.
E-mail address: pczhang@imm.ac.cn (P.-c. Zhang).

https://doi.org/10.1016/j.bioorg.2018.12.032
Received 21 September 2018; Received in revised form 30 November 2018; Accepted 22 December 2018
Available online 27 December 2018
0045-2068/ © 2018 Elsevier Inc. All rights reserved.

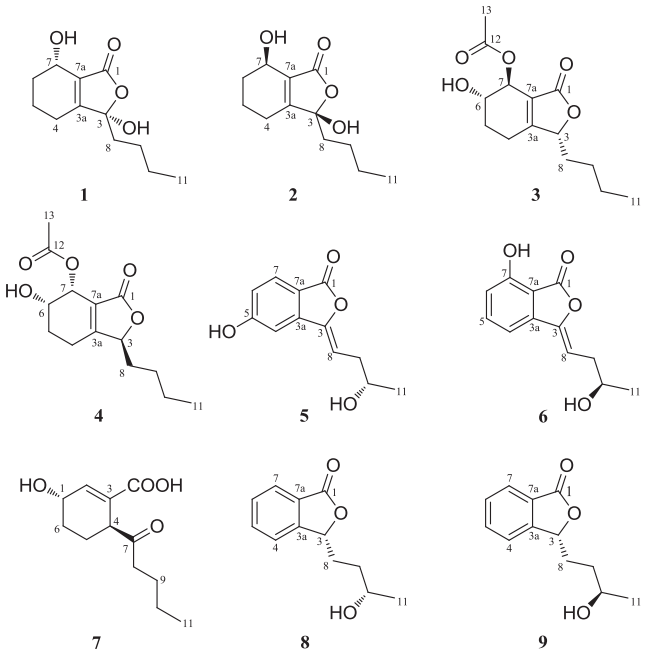

Fig. 1. Chemical structures of **1–9.**

2.2. Plant material

Roots of *Ligusticum chuanxiong* Hort. were collected from Pengzhou Town, Sichuan Province, PRC in June 2013 and identified by Professor Lin Ma. A voucher specimen (ID-S-2594) was deposited at the Institute of Materia Medica, Peking Union Medical College and Chinese Academy of Medical Sciences, Beijing, China.

2.3. Extraction and isolation

Powdered rhizome of *L. chuanxiong* Hort. (100.0 kg) was exhaustively extracted with 80% EtOH under reflux conditions. The solvent was evaporated by reduced pressure, and then, the residue (23.1 kg) was successively partitioned between EtOAc and *n*-BuOH. The EtOAc-soluble portion (5.0 kg) was chromatographed on a silica gel column and eluted with petroleum ether/ethyl acetate (gradient from 100:0 to 50:50) to produce 10 fractions (Ea − Ej) based on HPLC and TLC analyses. Fraction Ej (179.3 g) was separated on a silica gel column and eluted with petroleum ether/ethyl acetate (gradient from 100:1 to 1:10) to provide 10 fractions (Ej1 − Ej10) based on HPLC and TLC analyses. Fraction Ej5 (37.0 g) was chromatographed over Sephadex LH-20 and eluted with dichloromethane/MeOH (2:1) to yield 6 fractions (Ej5.1 − Ej5.6) based on HPLC and TLC analyses.

Ej5.3 (29.7 g) was chromatographed over an RP-C_{18} column and eluted with H_2O/MeOH (gradient from 9:1 to 1:4) to generate 15 fractions (Ej5.3.1 − Ej5.3.15) on the basis of HPLC and TLC analyses. Ej5.3.2 was further purified by preparative HPLC (MeCN/H_2O, 25:75, v/v, HOAc, 0.2%) to yield **5** (2.0 mg). Ej5.3.4 was further purified by preparative HPLC (MeCN /H_2O, 25:75, v/v, HOAc, 0.2%) to give the mixture of **8** and **9**. This mixture was further separated via a chiral column on preparative HPLC (MeCN/H_2O, 60:40, v/v, HOAc, 0.2%) to afford **8** (17.0 mg) and **9** (6.3 mg). Ej5.3.5 was further purified by preparative HPLC (MeOH/H_2O, 45:55, v/v, HOAc, 0.2%) to yield **6** (1.7 mg) and **7** (2.9 mg). Ej5.3.6 was purified by preparative HPLC (MeCN /H_2O, 25:75, v/v, HOAc, 0.2%) to produce a mixture of **1** and **2**. This mixture was further separated by use of a chiral column on preparative HPLC (MeCN/H_2O, 20:80, v/v, HOAc, 0.1%) to provide **1** (14.8 mg) and **2** (22.7 mg). Ej5.3.8 was purified by preparative HPLC (MeOH/H_2O, 45:55, v/v, HOAc, 0.2%) to isolate **3** (3.1 mg) and **4** (11.6 mg).

Table 1
^{1}H NMR (500 MHz) and ^{13}C NMR (125 MHz) data of compounds **1–4**.

Position	**1**, **2**[a]		**3**[b]		**4**[b]	
	δ_H (*J* in Hz)	δ_C	δ_H (*J* in Hz)	δ_C	δ_H (*J* in Hz)	δ_C
1		169.8		174.8		173.8
3		106.8	5.07, dd (3.0, 7.0)	84.6	5.03, dt (3.0, 7.5)	84.5
3a		164.9		170.0		172.0
4	2.07, m; 2.24, m	21.7	2.42, m	20.6	2.48, m	21.1
5	1.71,overlap	16.7	2.06, m	22.2	1.95, overlap	27.0
6	1.71,overlap; 1.51, m	31.3	4.27, m	62.3	3.97, m	68.7
7	4.26, brs	57.9	5.04, dd (3.0, 7.0)	73.2	5.45, dd (1.5, 4.5)	67.9
7a		128.8		126.5		123.9
8	1.67, overlap; 1.83, m	35.7	1.97, m; 1.58, m	32.5	1.95, overlap; 1.55, m	32.9
9	1.10, m	24.8	1.31, m	27.2	1.38, overlap	27.9
10	1.25, m	22.0	1.38, m	23.6	1.38, overlap	23.6
11	0.84, t (7.5)	13.9	0.93, t (7.0)	14.5	0.94, t (7.0)	14.4
12				171.9		172.1
13			2.07, s	21.0	2.07, s	21.0

[a] Measured in DMSO-d_6.
[b] Measured in methanol-d_4.

3. Results and discussion

Compound **1** and **2** are enantiomers. They were successfully separated by utilizing a reversed phase chiral column. Their optical rotations were determined to be −53 (*c* 0.1, MeOH) and +61 (*c* 0.1, MeOH), respectively. The negative HRESIMS gave the $[M-H]^-$ ion peak at *m/z* 225.1142, in accordance with the molecular formula of $C_{12}H_{18}O_4$. Their IR spectra indicated the presence of a carbonyl group (1746 cm^{-1}) and hydroxyl group (3192 cm^{-1}). The ^{1}H NMR spectra of **1** and **2** (Table 1) presented six methylene resonance signals at δ_H 2.24 (1H, m, H-4a), 2.07 (1H, m, H-4b), 1.71 (2H, overlap, H-5), 1.71 (1H, overlap, H-6a), 1.51 (1H, m, H-6b), 1.83 (1H, m, H-8a), 1.67 (1H, overlap, H-8b), 1.10 (2H, m, H-9), and 1.25 (2H, m, H-10); an oxymethine proton at δ_H 4.26 (1H, brs, H-7); and a methyl peak at δ_H 0.84 (3H, t, J = 7.5 Hz, H-11). The ^{13}C NMR spectra (Table 1) presented 12 carbons, including a carbonyl carbon (δ_C 169.8), two olefinic carbons (δ_C 164.9 and 128.8), a quaternary carbon (δ_C 106.8), an oxymethine carbon (δ_C 57.9), a methyl carbon (δ_C 13.9), and six methylene carbons. The above information suggested that compounds **1** and **2** may be tetrahydrobutylphthalides. According to the correlations of H-7/C-1, H-6/C-7a, H-4/C-7a, H-8/C-3a, H-10/C-8, and H-11/C-9 in the HMBC spectrum and H-4/H-5, H-5/H-6, H-6/H-7, H-11/H-10, and H-10/H-9 in the ^{1}H–^{1}H COSY spectrum (Fig. 2), a tetrahydrobutylphthalide skeleton was confirmed. Remarkably, a hydroxyl was confirmed and attached at the quaternary carbon according to the chemical shift of quaternary carbon (δ_C 106.8) and the HRESIMS information.

Therefore, the compounds **1** and **2** are enantiomers and their absolute configurations possess two pairs of potential forms: 3*S*,7*S*, 3*R*,7*R* and 3*S*,7*R*, 3*R*,7*S*. Through the use of the ECD calculations, four potential absolute configurations were calculated. Conformational analyses were carried out via systematic searching using a MMFF94 force field. The optimized conformations were obtained using the time-dependent density functional theory (TD-DFT) method at the B3LYP/6-31G(d) level. The overall calculated ECD spectra were generated by the Boltzmann weighting of the lowest energy conformers. Throughout the entire range of wavelengths, the calculated spectrum of 3*S*,7*S* matched the experimental data for **1** and the calculated spectrum of 3*R*,7*R* matched the experimental data for **2** (Fig. 4). Therefore, the structures of **1** and **2** were established and named ligusticumolide A and ligusticumolide B, respectively.

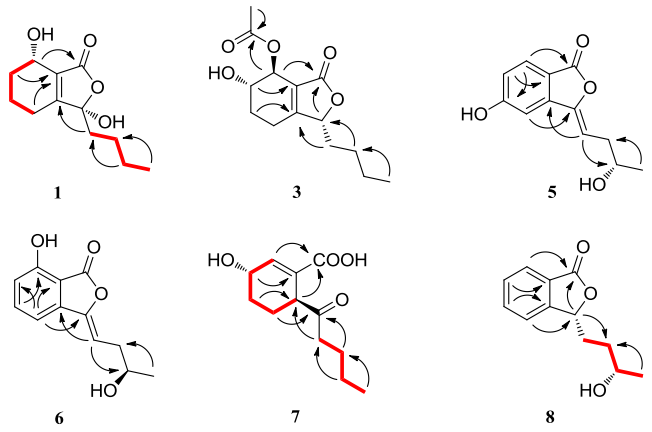

Fig. 2. Key HMBC (\) and ^{1}H–^{1}H COSY (\) correlations of **1–9.**

Compound **3** was obtained as a colorless oil. The molecular formula was determined to be $C_{14}H_{20}O_5$ by HRESIMS, implying 5 degrees of unsaturation. The IR spectrum vibrational peaks at 1730 cm^{-1} and 1648 cm^{-1} suggested the presence of γ-lactone and acyl groups. In the ^{1}H NMR spectrum (Table 1), a butyl chain [δ_H 1.97 (1H, m, H-8a), 1.58 (1H, m, H-8b), 1.31 (2H, m, H-9), 1.38 (2H, m, H-10) 0.93 (3H, t, J = 7.0 Hz, H-11)] was presented. Additionally, two methylenes [δ_H 2.42 (2H, m, H-4), 2.06 (2H, m, H-5)], three oxymethines [δ_H 5.07 (1H, dd, J = 3.0, 7.0 Hz, H-3), 4.27 (1H, m, H-6), 5.04 (1H, dd, J = 3.0, 7.0 Hz, H-7)] and one methyl [δ_H 2.07 (3H, s, H-13)] were also presented. The ^{13}C NMR spectrum (Table 1) displayed two olefinic carbons (δ_C 170.0 and 126.5), two carbonyl carbons (δ_C 174.8 and 171.9), and three oxymethine carbons (δ_C 84.6, 73.2 and 62.3). The remaining seven carbons represented five methylenes and two methyls. Obviously, compound **3** possessed the characteristic group of butylphthalide.

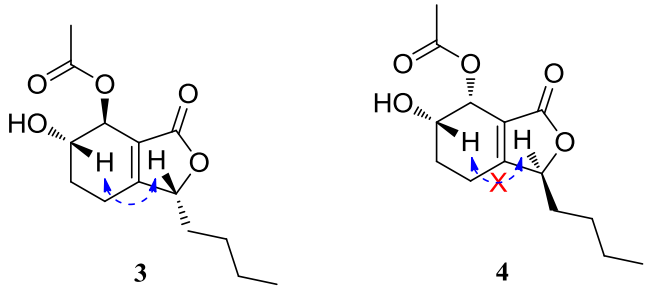

Fig. 3. Key ROESY(\) correlations of **3–4.**

However, compound **3** possessed 14 carbons rather than the typical 12 carbons of butylphthalide. According to the vibrational peaks at 1648 cm^{-1} of the IR spectrum and NMR data [δ_H 2.07 (3H, s, H-13); δ_C 171.9 (C-12)], an acetyl group was confirmed. In the HMBC spectrum (Fig. 2), the correlation of H-7/C-12 indicated that the acetyl group was attached at C-7. In addition, the correlations of H-3/C-1, H-5/C-3a, H-6/C-7a, H-7/C-1, H-8/C-3a, H-7/C-3a, H-7/C-12, and H-11/C-9 confirmed the tetrahydrobutylphthalide skeleton of **3**.

Mosher's method was used to determine the absolute configuration of C-6. According to the $\Delta\delta_H$ (δ_S-δ_R) values of H-5 ($\Delta\delta_H$ −0.049) and H-7 ($\Delta\delta_H$ +0.073), the absolute configuration of C-6 was confirmed to be *S* (see SI Fig. 18). Furthermore, according to the relatively large coupling constant (J = 7.0 Hz) between H-6 and H-7, the relative configuration of these atoms was confirmed to be *trans* [14]. Therefore, the absolute configuration of C-7 was confirmed to be *S*. In the ROESY experiment (Fig. 3), the correlation of H-3/H-6 indicated that they were on the same side. Therefore, the absolute configuration of C-3 was confirmed to be *R*. Thus, the structure of **3** was defined as shown and named ligusticumolide C.

Compound **4** had the same molecular formula as **3** according to HRESIMS ([M + Na]$^+$ 291.1204): $C_{14}H_{20}O_5$. The similar data of HRESIMS, IR, UV, and NMR suggested that **4** and **3** were isomers, with the difference being the absolute configuration. Through Mosher's method, the absolute configuration of C-6 was also confirmed to be *S* (see SI Fig. 28). However, the relatively small coupling constant (J = 4.5 Hz) (Table 1) between H-6 and H-7 suggested that this relative configuration was *cis* [14]. Therefore, the absolute configuration of C-7 was confirmed to be *R*. Meanwhile, there was no correlation between H-3 and H-6 in the ROESY spectrum (Fig. 3). Therefore, they were on different sides and the absolute configuration of C-3 was further confirmed to be *S*. Finally, the structure of **4** was confirmed as shown and named ligusticumolide D.

Compound **5** was obtained as a colorless oil with $[\alpha]_D^{20}$ −11 (*c* 0.05, MeOH). It was determined to have the molecular formula $C_{12}H_{12}O_4$ based on HRESIMS data ([M + H]$^+$ 221.0810). The IR absorption bands at 3392, 1754, 1607, and 1468 cm^{-1} indicated the presence of hydroxyl, lactone carbonyl, and aromatic ring functional groups, respectively. The ^{1}H NMR data (Table 2) showed resonances that were characteristic of an ABX system of a benzene ring at δ_H 7.08 (1H, d, J = 2.0 Hz, H-4), 6.97 (1H, dd, J = 8.5, 2.0 Hz, H-6), and 7.67 (1H, d, J = 8.5 Hz, H-7) and a butenyl chain at δ_H 5.76 (1H, t, J = 7.5 Hz, H-8), 2.55 (2H, m, H-9), 3.93 (1H, m, H-10), and 1.23 (3H, d, J = 6.0 Hz, H-11). The above information presented the characteristic signals of butenylphthalide and was further verified according to the 12 carbon skeleton in the ^{13}C NMR spectrum (Table 2). The HMBC correlations (Fig. 2) H-7/C-5, H-6/C-7a, H-4/C-3, H-8/C-10, and H-11/

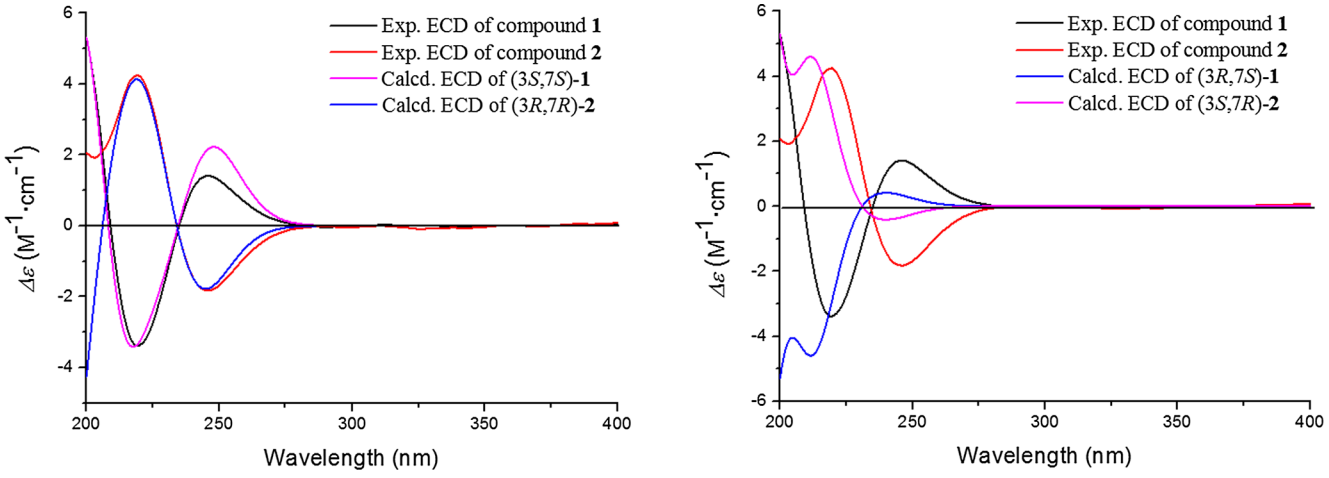

Fig. 4. Experimental ECD and calculated ECD spectrum of **1** and **2** in MeOH.

Table 2
^{1}H NMR (500 MHz) and ^{13}C NMR (125 MHz) data of compounds **5–7** in methanol-d_4.

Position	5		6		7	
	δ_H (J in Hz)	δ_C	δ_H (J in Hz)	δ_C	δ_H (J in Hz)	δ_C
1		168.8		167.9	4.27, m	66.3
2					6.99, brs	144.2
3		148.1		148.3		132.9
3a		143.7		142.6		
4	7.08, d (2.0)	106.5	7.21, d (8.0)	111.7	3.61, m	49.1
5		165.8	7.53, t (8.0)	138.0	2.11, m; 1.52, m	24.2
6	6.97, dd (2.0, 8.5)	119.8	6.86, d (8.0)	117.6	1.92, m; 1.52, m	30.5
7	7.67, d (8.5)	127.9		158.8		214.6
7a		116.6		111.5		
8	5.76, t (7.5)	106.3	5.79, t (7.5)	106.2	2.62, m	42.1
9	2.55, m	36.4	2.55, m	36.4	1.51, m	26.9
10	3.93, m	68.2	3.93, m	68.3	1.31, m	23.4
11	1.23, d (6.0)	23.4	1.22, d (6.0)	23.3	0.91, t (7.5)	14.4
–COOH						170.2

C-9 implied the presence of two –OH groups at C-5 and C-10. The $Rh_2(OCOCF_3)_4$-induced ECD method was conducted to determine the absolute configuration of **5**. By treating **5** with $Rh_2(OCOCF_3)_4$ in anhydrous CH_2Cl_2, a positive Cotton effect at 359 nm in the ECD spectrum was observed for the complex (see SI Fig. 39) [15]. According to the bulkiness rule, the absolute configuration of C-10 was determined to be *S*. Therefore, compound **5** was established as shown and named ligusticumolide E.

Compound **6** had the same molecular formula, $C_{12}H_{12}O_4$, as compound **5** according to the HRESIMS data (m/z 221.0793 $[M + H]^+$). However, there was an ABC benzene ring system at δ_H 7.53 (1H, t, J = 8.0 Hz, H-5), 7.21 (1H, d, J = 8.0 Hz, H-4), and 6.86 (1H, d, J = 8.0 Hz, H-6) in the ^{1}H NMR spectrum (Table 2) of **6** instead of the ABX system as in **5**. In the HMBC spectrum (Fig. 2), the correlations of H-5/C-7, H-4/C-6, H-4/C-7a, H-8/C-10 and H-11/C-9 indicated the presence of two –OH groups at C-7 and C-10. By comparing the specific rotations of **5** (−11 *c* 0.05, MeOH) and **6** (+14 *c* 0.05, MeOH), the absolute configuration of C-10 was determined to be *R* in **6**. Thus, compound **6** was confirmed as shown and named ligusticumolide F.

Compound **7** was obtained as a colorless crystal, $[\alpha]_D^{20}$ +31 (*c* 0.10, MeOH). Its molecular formula, $C_{12}H_{18}O_4$, which possessed 4 degrees of unsaturation, was determined from the HRESIMS data. The IR spectrum suggested the presence of carbonyl (1710 cm^{-1}) and carboxyl (1659 cm^{-1}) groups, which was confirmed by the ^{13}C NMR data [δ_C 214.6 (C-7); 170.2 (C-COOH)]. In the ^{13}C NMR spectrum (Table 2), the signals of δ_C 144.2 (C-2) and δ_C 132.9 (C-3) indicated that **7** possessed a double bond functional group in accordance with the signal of δ_H 6.99 (1H, brs, H-2) in the ^{1}H NMR spectrum (Table 2). According to the 4 degrees of unsaturation of compound **7**, there was only one remaining degree of unsaturation, which suggested the presence of a ring. This was clarified by the correlations of H-2/C-4, H-1/C-3, and H-6/C-4 in the HMBC spectrum and H-2/H-1, H-1/H-6, H-6/H-5, and H-5/H-4 in the ^{1}H–^{1}H COSY spectrum (Fig. 2). In the ^{1}H NMR spectrum (Table 2), the resonances at δ_H 0.91 (3H, t, J = 7.5 Hz, H-11), 1.31 (2H, m, H-10), 1.51 (2H, m, H-9), and 2.62 (2H, m, H-8) showed the presence of a butyl chain. The carbonyl group was attached at C-7 on the basis of the correlations of H-9/C-7, H-8/C-4, and H-5/C-7, and the carboxyl group was attached at C-3 on the basis of the correlations of H-2/–COOH, and H-4/–COOH in the HMBC spectrum (Fig. 2). Therefore, the planar structure of **7** was confirmed to be an analogue of tetrahydrobutylphthalide. The absolute configuration of **7** was determined by the ECD calculation method. Compound **7** included two pairs of potential absolute configurations: 1*R*,4*R*, 1*S*,4*S* and 1*S*,4*R*, 1*R*,4*S*. Because the relative configuration of **7** could not be determined through NMR experiments, two pairs of potential absolute configurations were calculated. Throughout the entire range of wavelengths, the calculated spectrum of 1*S*,4*S* matched with the experimental data for **7** (Fig. 5). Thus, the structure of compound **7** was confirmed as shown and named ligusticumolide G.

Compounds **8** and **9** were first reported by a patent in China [16]. However, their structures were not assigned in this patent. Here, their structures were assigned through HRESIMS and NMR data. Compound **8** was obtained as a colorless oil with $[\alpha]_D^{20}$ −53 (*c* 0.10, MeOH). Through the HRESIMS data ($[M + H]^+$ m/z 207.1009), its molecular formula was confirmed to be $C_{12}H_{14}O_3$. The ^{1}H NMR data (Table 3) indicated a benzene ring at δ_H 7.84 (1H, d, J = 8.0 Hz, H-7), 7.58 (1H, t, J = 8.0 Hz, H-6), 7.75 (1H, t, J = 8.0 Hz, H-5), 7.61 (1H, d, J = 8.0 Hz, H-4). In addition, a butyl chain was presented at δ_H 2.28 (1H, m, H-8a), 1.74 (1H, m, H-8b), 1.50 (1H, m, H-9a), 1.56 (1H, m, H-9b), 3.74 (1H, m, H-10), and 1.15 (3H, d, J = 6.5 Hz, H-11); this was clarified by the correlations of H-11/H-10, H-10/H-9, and H-9/H-8 in the ^{1}H–^{1}H COSY spectrum (Fig. 2). According to the above information, compound **8** was confirmed to be a typical butylphthalide. Its structure was further assigned by the correlations of H-3/C-1, H-4/C-3, H-5/C-3a, H-6/C-7a, H-7/C-1, H-3/C-9, and H-11/C-9 in the HMBC spectrum (Fig. 2). Using Mosher's method, the absolute configuration of C-10 was confirmed to be *S* [H-9 ($\Delta\delta_H$ +0.229) and H-11 ($\Delta\delta_H$ −0.082)] (see SI Fig. 60). The ECD calculation method was carried out to determine the

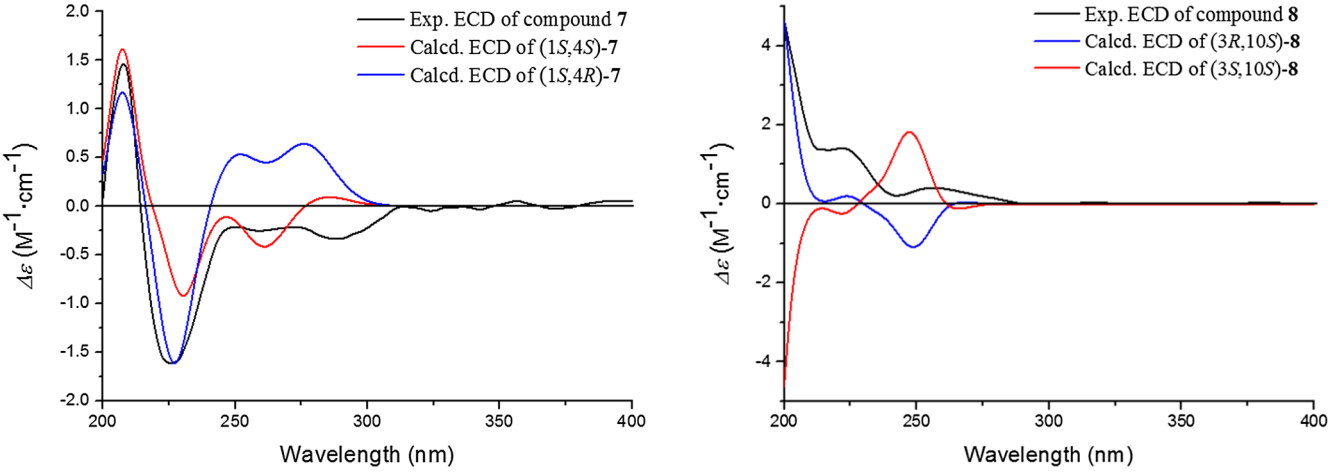

Fig. 5. Experimental ECD and calculated ECD spectrum of **7** and **8** in MeOH.

Table 3
^{1}H NMR (500 MHz) and ^{13}C NMR (125 MHz) data of compounds **8–9** in methanol-d_4.

Position	8		9	
	δ_H (J in Hz)	δ_C	δ_H (J in Hz)	δ_C
1		172.8		172.9
3	5.61, dd (4.0, 7.5)	83.5	5.63, dd (4.0, 7.5)	83.2
3a		151.9		151.9
4	7.61, d (8.0)	123.6	7.61, d (8.0)	123.6
5	7.75, t (8.0)	135.7	7.76, t (8.0)	135.7
6	7.58, t (8.0)	130.5	7.58, t (8.0)	130.5
7	7.84, d (8.0)	126.4	7.84, d (8.0)	126.4
7a		127.2		127.2
8	2.28, m; 1.74, m	32.2	2.16, m; 1.88, m	32.0
9	1.50, m; 1.56, m	35.2	1.45, m; 1.56, m	35.0
10	3.74, m	68.3	3.78, m	68.0
11	1.15, d (6.5)	23.7	1.15, d (6.0)	23.7

absolute configuration of C-3. As a result, the calculated spectrum of 3*R*,10*S* matched the experimental data for **8** (Fig. 5). Finally, the structure of **8** was completely assigned as shown.

The identical assignment procedure was used to confirm the structure of compound **9**. The primary difference between **9** and **8** was their absolute configuration. The absolute configuration of C-10 was confirmed to be *R* [H-9 ($\Delta\delta_H$ −0.200) and H-11 ($\Delta\delta_H$ +0.056)] in compound **9** (see SI Fig. 68). According to the specific rotations of **9** (−58 *c* 0.10, MeOH) and **8** (−53 *c* 0.10, MeOH), they were confirmed to be diastereomers. Therefore, the absolute configuration of C-3 was determined to be *R* in **9**. Thus, the structure of **9** was also completely assigned, as shown.

All of the compounds were tested for their neuroprotective effects against SH-SY-5Y cell injury induced by H_2O_2. The results showed that none of the compounds exhibited neuroprotective effects. In addition, all of the compounds were also assayed for their hepatoprotective activities. Compared with the control group, compounds **4**, **5**, and **7–9** showed significant hepatoprotective activity against APAP-induced HepG2 cell injury (Fig. 6).

4. Structure characterization

Ligusticumolide A (1). Colorless oil; UV λ_{max} (MeOH) (log ε): 209 (3.96) nm; $[\alpha]_D^{20}$ −53 (*c* 0.1 MeOH); HRESIMS *m/z* 225.1142 $[M-H]^-$ (calcd 225.1132); IR ν_{max}: 3299, 2959, 1746, 1687, 1481, 1373, 1267, 1074, 990, 921, 900 cm^{-1}; ^{1}H NMR and ^{13}C NMR see Table 1.

Ligusticumolide B (2). Colorless oil; UV λ_{max} (MeOH) (log ε): 209 (3.96) nm; $[\alpha]_D^{20}$ +61 (*c* 0.1 MeOH); HRESIMS *m/z* 225.1142 $[M-H]^-$ (calcd 225.1132); IR ν_{max}: 3299, 2959, 1746, 1687, 1481, 1373, 1267, 1074, 990, 921, 900 cm^{-1}; ^{1}H NMR and ^{13}C NMR see Table 1.

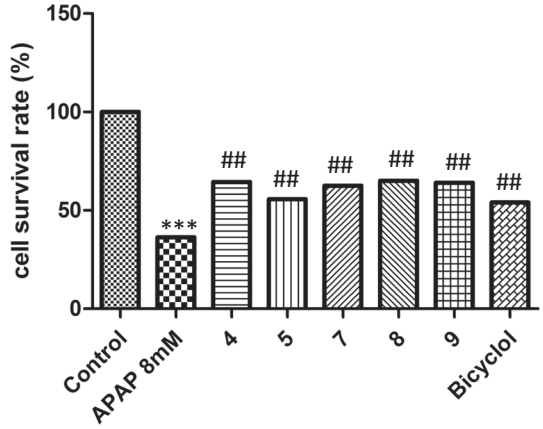

Fig. 6. Hepatoprotective effects of compounds **4**, **5**, and **7–9** (10 μM) against APAP (8 mM)-induced HepG2 cell injury. $^{***}p < 0.001$, $^{\#\#}p < 0.01$.

Ligusticumolide C (3). Colorless oil; UV λ_{max} (MeOH) (log ε): 213 (4.24) nm; $[\alpha]_D^{20}$ −54 (*c* 0.1 MeOH); HRESIMS *m/z* 291.1204 $[M+Na]^+$ (calcd 291.1203); IR ν_{max}: 3282, 2922, 1730, 1648, 1541, 1238, 1045 cm^{-1}; ^{1}H NMR and ^{13}C NMR see Table 1.

Ligusticumolide D (4). Colorless oil; UV λ_{max} (MeOH) (log ε): 212 (4.24) nm; $[\alpha]_D^{20}$ −114 (*c* 0.1 MeOH); HRESIMS *m/z* 291.1203 $[M+Na]^+$ (calcd 291.1203); IR ν_{max}: 3425, 2932, 1757, 1679, 1372, 1232, 1041, 961 cm^{-1}; ^{1}H NMR and ^{13}C NMR see Table 1.

Ligusticumolide E (5). Colorless oil; UV λ_{max} (MeOH) (log ε): 256 (4.30) nm; $[\alpha]_D^{20}$ −11 (*c* 0.05 MeOH); HRESIMS *m/z* 221.0810 $[M+H]^+$ (calcd 221.0808); IR ν_{max}: 3392, 2971, 1754, 1607, 1468, 1296, 1075, 1047, 934 cm^{-1}; ^{1}H NMR and ^{13}C NMR see Table 2.

Ligusticumolide F (6). Colorless oil; UV λ_{max} (MeOH) (log ε): 225 (4.23), 264 (3.98), 333 (3.78) nm; $[\alpha]_D^{20}$ +14 (*c* 0.05 MeOH); HRESIMS *m/z* 221.0793 $[M+H]^+$ (calcd 221.0808); IR ν_{max}: 3344, 2971, 1755, 1606, 1473, 1299, 1015, 809, 695 cm^{-1}; ^{1}H NMR and ^{13}C NMR see Table 2.

Ligusticumolide G (7). Colorless crystal; UV λ_{max} (MeOH) (log ε): 206 (3.79) nm; $[\alpha]_D^{20}$ +31 (*c* 0.10 MeOH); HRESIMS *m/z* 227.1252 $[M+H]^+$ (calcd 227.1278); IR ν_{max}: 3379, 2952, 2617, 1710, 1659, 1404, 1261, 1108, 1043, 1008, 918, 697 cm^{-1}; ^{1}H NMR and ^{13}C NMR see Table 2.

Neuroprotective Activities Assay. Human neuroblastoma SH-SY5Y cells were maintained in DMEM supplemented with 10% FBS, 100 U/mL penicillin and 100 μg/mL streptomycin at 37 °C under a water-saturated atmosphere of 95% air and 5% CO_2. Cells were seeded in 96-well culture plates in 100 μL for 18 h, then incubated with isolated compounds (10 μL, 10 μM) for 4 h. In order to induce an oxidative stress, 100 μL H_2O_2 freshly prepared was added to the cells and incubated with the compounds at 37 °C for 24 h. Then 10 μL MTT solution (5 mg/mL) was added into each well and incubated for 4 h at 37 °C. Cells were finally lysed with 150 μL DMSO. The absorbance was measured at 570 nm, using edaravone as the positive control. Results were expressed as percentage of cell viability (%), hypothesizing control cells as 100%.

Hepatoprotective Activities Assay. The HepG2 cell line was maintained in DMEM containing 10% FBS and penicillin (100 U/mL) − streptomycin (100 μg/mL) and cultured at 37 °C (5% CO_2, 100% relative humidity). These cells were digested using 0.25% trypsin and then seeded into 96-well plates. After incubation for 12 h, the cells in the 96-well plates were treated with different samples (10 μM) and APAP (8 mM), and the samples were incubated for 48 h. Then, 100 μL of MTT reagent (0.5 mg/mL) was added to each well and incubated for 4 h. After removal of the media, 150 μL of DMSO was added to solubilize the residuum. Finally, the absorbances were measured at 570 nm, using bicyclol as the positive control.

Acknowledgements

This work was supported by the National Natural Science Foundation of China (No. 81773588) and CAMS Innovation Fund for Medical Sciences (CIFMS) (No. 2016-I2M-1-010).

Appendix A. Supplementary material

Supplementary data to this article can be found online at https://doi.org/10.1016/j.bioorg.2018.12.032.

References

[1] G. Lin, S.S.K. Chan, H.S. Chung, S.L. Li, Stud. Nat. Prod. Chem. 32 (2005) 611–669.
[2] W.X. Li, Y.P. Tang, Y.Y. Chen, J.A. Duan, Molecules 17 (2012) 10614–10651.
[3] Z.J. Chen, C. Zhang, F. Gao, Q. Fu, C.M. Fu, Y. He, J.M. Zhang, Food Chem. Toxicol.

119 (2018) 309–325.
[4] S. Wang, F. Ma, L.J. Huang, Y. Zhang, Y.C. Peng, C.H. Xing, Y.P. Feng, X.L. Wang, Y. Peng, CNS Neurol. Disord.-Dr. 17 (2018) 338–347.
[5] J. Huang, X.Q. Lu, C. Zhang, J. Lu, G.Y. Li, R.C. Lin, J.H. Wang, Fitoterapia 91 (2013) 21–27.
[6] J. Huang, X.Q. Lu, J. Lu, G.Y. Li, H.Y. Wang, L.H. Li, R.C. Lin, J.H. Wang, J. Asian Nat. Prod. Res. 15 (2013) 1237–1242.
[7] M. Kim, S.O. Kim, M. Lee, J.H. Lee, W.S. Jung, S.K. Moon, Y.S. Kim, K.H. Cho, C.N. Ko, E.H. Lee, Eur. J. Pharmacol. 740 (2014) 504–511.
[8] J. Yang, X.L. Feng, Y. Yu, Q. Wang, J. Zou, C.X. Wang, Z.Q. Mu, X.S. Yao, H. Gao, Chin. Med. 11 (2016) 1–7.
[9] W. Wei, X.W. Wu, X.W. Yang, RSC Adv. 6 (2016) 61037–61046.
[10] W. Wei, W. Xu, X.W. Yang, J. Asian Nat. Prod. Res. 19 (2017) 1–8.
[11] X. Zhang, B. Han, Z.M. Feng, Y.Y. Yang, J.S. Jiang, P.C. Zhang, RSC Adv. 7 (2017) 37478–37486.
[12] X. Zhang, B. Han, Z.M. Feng, Y.Y. Yang, J.S. Jiang, P.C. Zhang, Fitoterapia 125 (2018) 147–154.
[13] X. Zhang, B. Han, Z.M. Feng, Y.Y. Yang, J.S. Jiang, P.C. Zhang, Org. Chem. Front. 5 (2018) 1423–1430.
[14] T. Naito, T. Katsuhara, K. Niitsu, Y. Ikeya, M. Okada, H. Mitsuhashi, Phytochemistry 31 (1992) 639–642.
[15] T.H. Zhu, H.G. Ma, C. Wang, C.Y. Zhao, X.G. Mei, W.M. Zhu, J. Int. Pharm. Res. 42 (2015) 773–785.
[16] W.J. Mi. Faming Zhuanli Shenqing (2016) CN 105267207 A.